Supporting Information

Ardiles et al. 10.1073/pnas.1201209109

SI Materials and Methods

Animals. *Octodon degus* were obtained from a breeding colony at the animal facility of the University of Valparaiso and maintained in a controlled temperature room (23 ± 1 °C), under a 12:12 light/dark cycle, with water and food provided ad libitum. At the time of behavioral characterization, degus of either sex were grouped by age: 6, 12, 36, and 60 mo old. For several experiments, 72-mo-old mice were used as well. Two behavioral tests were performed for memory characterization: object recognition memory (ORM) and spatial T-maze. Each behavioral session was videotaped for further analysis offline. The level of illumination measured at the ground level of the experimental arena produced by a fluorescence tube varied between 220 and 290 lux. All animals were housed in individual home cages from 3 d before the behavioral experimental sessions. All efforts were made to minimize animal discomfort and stress while also limiting the number of animals used.

Spatial Working Memory. A T-maze was constructed of black Plexiglas with two 18 × 23.5 × 50 cm arms and a starting area with a guillotine door measuring 18 × 20 cm. A recessed black glass cup (5 cm Ø, 1 cm deep) for food reward was placed on the floor at the end of each arm. To Animals' motivation for the task was encouraged by a food deprivation standard protocol, maintaining 85–90% of ad libitum weight during the experimental sessions.

Electrophysiology. Hippocampal slices were prepared from behaviorally tested degus. Animals were perfused intracardially with ice-cold dissection buffer (2.6 mM KCl, 1.23 mM NaH_2PO_4, 26 mM $NaHCO_3$, 212.7 mM sucrose, 10 mM dextrose, 3 mM $MgCl_2$, and 1 mM $CaCl_2$, equilibrated with 95% O_2 and 5% CO_2) under deep halothane anesthesia, and the brains were promptly removed. The hippocampus was removed and sectioned into 300- to 400-μm-thick slices using a vibratome (Vibratome 1000 Plus). The slices were transferred and maintained for 1 h at room temperature in normal artificial cerebrospinal fluid (ACSF), which was similar to the dissection buffer but with sucrose replaced by 124 mM NaCl, $MgCl_2$ lowered to 1 mM, and $CaCl_2$ raised to 2 mM. All recordings were done in a submersion recording chamber perfused with ACSF (30 ± 0.5 °C; 2 mL/min). Field excitatory postsynaptic potentials (fEPSPs) were evoked by stimulating the Schaffer collaterals with 0.2-ms pulses delivered through concentric bipolar stimulating electrodes (FHC) and recorded extracellularly in CA1 stratum radiatum. Baseline responses were recorded using half-maximum stimulation intensity at 0.033 Hz. Basal synaptic transmission was assayed by determining input–output relationships from fEPSPs generated by gradually increasing the stimulus intensity; the input was the peak amplitude of the fiber volley, and the output was the initial slope of the fEPSP. Paired-pulse facilitation was elicited using an interstimulus interval of 50–1,400 ms. Long-term potentiation (LTP) was induced by theta burst stimulation, consisting of four theta epochs delivered at 0.1 Hz. Each epoch in turn consisted of 10 trains of four pulses (at 100 Hz) delivered at 5 Hz. Long-term depression (LTD) was induced by paired-pulse low-frequency stimulation, consisting of 900 pulses at 1 Hz. These protocols were delivered after 20 min of stable baseline transmission.

Miniature excitatory postsynaptic currents (mEPSCs) were recording in visually identified CA1 pyramidal cells and patched using a whole-cell patch pipette (3–5 MΩ) filled with intracellular solution containing 120 mM KCl, 8 mM NaCl, 2 mM EGTA, 10 mM Hepes, 4 mM ATP, 0.5 mM GTP, 10 mM phosphocreatine, and 5 mM QX-314 (lidocaine *N*-ethyl bromide) (pH 7.4; 285–295 mOsm). To isolate AMPA receptor-mediated mEPSCs, 1 μM tetrodotoxin, 20 μM bicuculline, and 100 μM D,L-APV were added to the ACSF (2 mL/min, 30 ± 1 °C), which was continually bubbled with 95%O_2/5% CO_2. mEPSCs were recorded at a holding potential of –80 mV with an Axopatch-clamp amplifier (Molecular Devices) digitized at 2 kHz using a data acquisition board (National Instruments) and acquired using Igor Pro software (WaveMetrics). mEPSCs were then analyzed with the Mini Analysis program (Synaptosoft). The threshold for detecting mEPSCs was set at three times the rms of noise. There was no significant difference in the rms of noise between the experimental groups (young: 0.86 ± 0.081, n = 12; aged: 0.73 ± 0.081, n = 9). Cells showing a negative correlation between mEPSC amplitude and rise time (i.e., dendritic filtering present) were excluded from the analysis, as were mEPSCs with a >3-ms rise time (measured between 10% and 90% of amplitude). Average mEPSC amplitude and frequency were calculated and compared across different experimental groups using the unpaired Student t test. Only cells and recording conditions that met the following criteria were studied: Vm = –65 mV, input R = 200 MΩ, and series R = 20 MΩ. Cells were discarded if input R or series R changed by more than 15%.

Immunoblot Analysis. After electrophysiological recording, hippocampal slices were promptly frozen in liquid nitrogen. Samples were homogenized in ice-cold lysis buffer [10 mM Tris-Cl (pH 7.4), 5 mM EDTA, 1% Nonidet P-40, 1% sodium deoxycholate, and 1% SDS), supplemented with a protease inhibitor mixture (1 mM PMSF, 2 mg/mL aprotinin, 1 mg/mL pepstatin, and 10 mg/mL benzamidine) and phosphatase inhibitors (25 mM NaF, 100 mM Na_3VO_4, 1 mM EDTA, and 30 mM $Na_4P_20_7$) using a Potter homogenizer. Protein samples were centrifuged twice for 5 min at 20,000 × g at 4 °C. Protein concentration was determined using the Pierce BCA Protein Assay Kit (Thermo Fisher Scientific). For synaptic proteins, 30 μg of protein per lane was resolved by 12% SDS/PAGE, followed by immunoblotting on Immobilon PVDF membranes (Millipore) using mouse anti-PSD95, mouse anti-GluR2, mouse anti-NR2b (University of California Davis/National Institutes of Health NeuroMab Facility), goat anti-synaptophysin, rabbit anti-actin, or rabbit anti–b-tubulin antibodies (Santa Cruz Biotechnology). For tau phosphorylation, samples were probed with phospho-tau–specific antibodies PHF-1 (University of California Davis/National Institutes of Health NeuroMab Facility) and AT8 (Thermo Fisher Scientific). For Aβ peptides, 80–100 μg of proteins were resolved in 17.5% SDS-polyacrylamide Tris-tricine gels, followed by immunoblotting on PVDF membranes using mouse anti-Aβ protein 4G8 (Chemicon). Band intensities were visualized by ECL (Pierce) and scanned and densitometrically quantified using ImageJ software. Soluble Aβ oligomers were measured by slot-blot assays as described previously (1). In brief, the total protein extract was centrifuged at 20,000 × g for 1 h to eliminate fibrillar aggregates. The protein concentration of the soluble fraction was determined, and 6 mg of protein was spotted in 0.45 mm^2 nitrocellulose (Millipore), blocked with PBS-T gelatin 0.4%, and incubated using an anti-oligomeric antibody A11 (Chemicon) at a 1:5,000 dilution for 4 h at 4 °C. Slot blots were then processed as described earlier.

Immunohistochemistry Procedures. Perfusion and fixation were performed as described previously (2, 3). Free-floating immunocytochemical procedures were performed as described previously

(3). Washing and dilution of immune reagents were performed using 0.01 M PBS with 0.2% Triton X-100 (PBS-T), with two PBS-T washes per antibody incubation. Sections were pretreated with 0.5% H_2O_2 for 30 min to reduce endogenous peroxidase activity, followed by treatment with 3% BSA at room temperature for 1 h to avoid nonspecific binding. Primary antibodies were incubated overnight at 4 °C. Primary antibodies were detected using the Pierce ABC Kit (Thermo Fisher Scientific). Staining was developed by a 15-min incubation with 0.6% diaminobenzidine, followed by the addition of H_2O_2 (0.01% final concentration). After immunostaining, all sections were mounted on gelatin-coated slides, air-dried, dehydrated, and cover-slipped with Canada balsam (Merck). The specific antibodies used for immunohistochemistry were anti-phosphorylated tau AT8 (recognizing Ser-199– and Ser-202–phosphorylated tau; 1:300) and anti-Aβ 6E10. The sections were pretreated with 0.3% H_2O_2 to eliminate endogenous peroxidase activity and then incubated in 3% BSA in PBS. All washes and antibody dilutions were done using 0.4% Triton X-100 in PBS. Immunohistochemistry was performed by the ABC (avidin-biotin-HRP complex) method (Vector Laboratories). Free-floating sections were mounted on gelatin-precoated slides, air-dried, dehydrated in graded ethanol, and covered with Canada balsam (Merck). Image analysis and PHF-1 neuronal counting were done as described previously (4).

Thioflavin-S Staining. Thioflavin-S (ThS) staining was developed in sections mounted on gelatin-coated slices as described previously (1, 5). After dehydration and rehydration in ethanol and xilol batteries, slices were incubated in distilled water for 10 min and then immersed in the ThS solution (0.1% ThS in 70% ethanol) for 5 min. Slices were then washed twice in 70% ethanol for 30 s and cover-slipped with antifade mounting medium in dark.

Image Analysis. Stained brain sections were photographed with an Olympus BX51 microscope coupled to a Micropublisher 3.3 RTV camera (QImaging). The luminance of the incident light and the time of exposure were calibrated to assign pixel values ranging from 0 to 255 in RGB images (no-light to full-light transmission), which were used for all preparations. The images were loaded into ImageJ software for analysis. Areas for measurement were selected by manual threshold adjustment or direct manual selection of regions of interest in heterogeneous stains.

Principal Components Analysis. We performed multivariate principal components analysis to reduce the dimensionality of the database. In this analysis, eigenvalue decomposition of the covariance matrix of the data after mean centering of each variable results in a set of uncorrelated variables ordered by the amount of explained variance in the data. Consequently, the internal structure of the data can be satisfactorily observed in lower dimensionality (using only the first principal component). This simple linear transformation can be useful for visualization as well as for deeper analysis, providing ready access to the projection of data and variables herein.

1. Toledo EM, Inestrosa NC (2010) Activation of Wnt signaling by lithium and rosiglitazone reduced spatial memory impairment and neurodegeneration in brains of an APPswe/PSEN1DeltaE9 mouse model of Alzheimer's disease. *Mol Psychiatry* 15:272–285.
2. De Ferrari GV, et al. (2003) Activation of Wnt signaling rescues neurodegeneration and behavioral impairments induced by beta-amyloid fibrils. *Mol Psychiatry* 8:195–208.
3. Reyes AE, et al. (2004) Acetylcholinesterase-Abeta complexes are more toxic than Abeta fibrils in rat hippocampus: Effect on rat beta-amyloid aggregation, laminin expression, reactive astrocytosis, and neuronal cell loss. *Am J Pathol* 164: 2163–2174.
4. Cancino GI, et al. (2008) STI571 prevents apoptosis, tau phosphorylation and behavioural impairments induced by Alzheimer's beta-amyloid deposits. *Brain* 131: 2425–2442.
5. Chacón MA, Barría MI, Soto C, Inestrosa NC (2004) Beta-sheet breaker peptide prevents Abeta-induced spatial memory impairments with partial reduction of amyloid deposits. *Mol Psychiatry* 9:953–961.

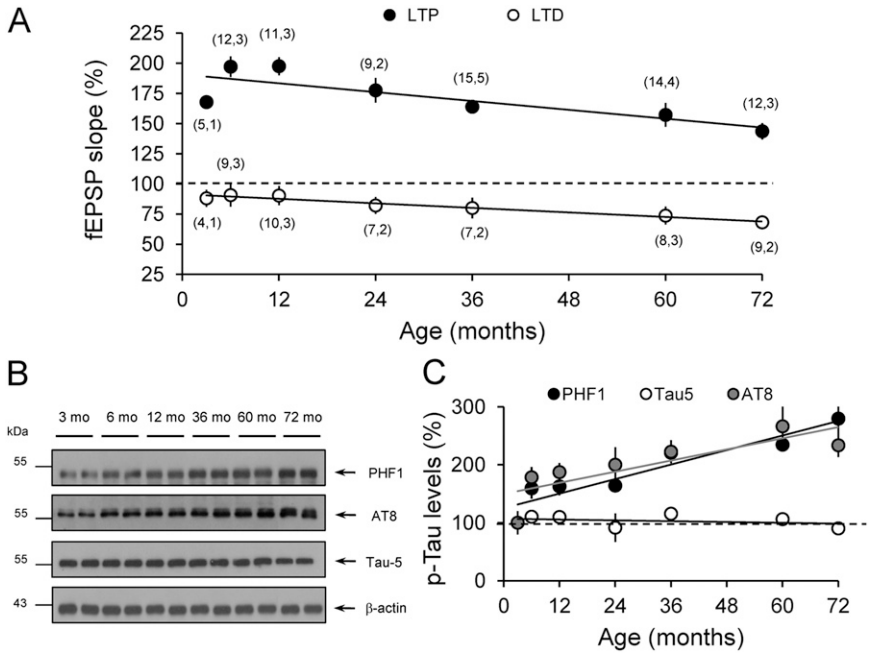

Fig. S1. Age profile of synaptic plasticity in *O. degus*. (*A*) Progression of age-related changes in hippocampal LTP (black) and LTD (white). Averaged LTP and LTD magnitude were determined 1 h after application of the induction protocols. LTP declined, whereas LTD increased linearly with age ($r = -0.82$ for LTP; $r = -0.98$ for LTD). (*B*) Age-dependent increase in phosphorylated tau levels assessed by WB. (*C*) Semiquantification of phosphorylated tau levels (relative to β-tubulin levels) expressed as a percentage of respective averaged signals observed in 3-mo-old degus. Phosphorylated tau levels increased linearly with age, whereas total tau levels remained unchanged ($r = 0.94$ for PHF1, $r = 0.82$ for AT8, $r = -0.33$ for Tau-5). The number of experiments is indicated in parentheses.

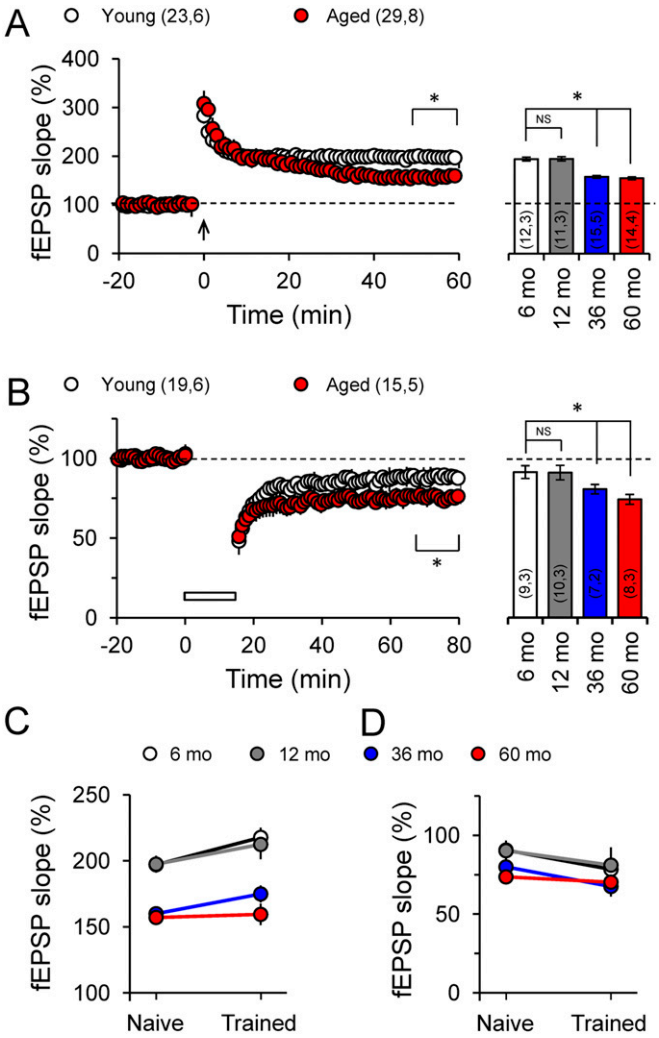

Fig. S2. Training does not modify the induction or maintenance of long-term synaptic plasticity in the Schaffer collateral–CA1 synapse in *O. degus*. (*A*) Theta-burst stimulation-induced LTP from untrained young (white) and aged (red) degus. The LTP protocol was delivered at the time indicated by the arrow. Two-way ANOVA [$F_{(1,10)}$ = 1,472, *P < 0.0001], followed by the Bonferroni post hoc test (P < 0.05) in the last 10 min for aged vs. young. The averaged LTP magnitudes during the last 10 min of recording for 6-mo-old (white), 12-mo-old (gray), 36-mo-old (blue), and 60-mo-old (red) degus are also shown. Two-way ANOVA [$F_{(3,27)}$ = 327.9, *P < 0.0001] followed by the Bonferroni post hoc test (P < 0.05) in the last 10 min compared with 6 mo-old. (*B*) Paired-pulse low-frequency stimulation-induced LTD from untrained young (white) and aged (red) degus. LTD protocol was delivered at the time indicated by the horizontal open bar. Two-way ANOVA [$F_{(1,10)}$ = 266.9, *P < 0.0001], followed by the Bonferroni post hoc test (P < 0.05) in the last 10 min for aged vs. young. Averaged LTD magnitudes during the last 10 min of recording for 6-mo-old (white), 12-mo-old (gray), 36-mo-old (blue), and 60-mo-old (red) degus are also shown. Two-way ANOVA [$F_{(1,3)}$ = 11.71, *P < 0.0001], followed by the Bonferroni post hoc test (P < 0.05) on the last 10 min compared with 6 mo-old. Calibration: 1 mV, 10 ms. (*C* and *D*) Comparisons of LTP and LTD magnitude by age in naïve and trained degus. No differences were seen between naive and trained animals at any age (P = 0.485 for LTP; P = 0.200 for LTD, unpaired two-tailed t test). Values in parentheses indicate the number of hippocampal slices and number of animals used.

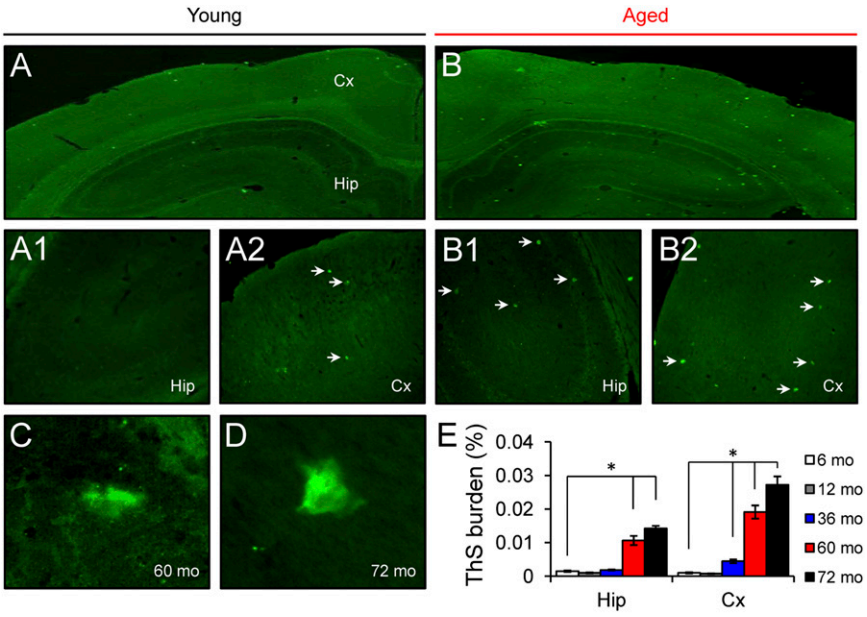

Fig. S3. Amyloid fibrilar deposition in the hippocampus and cerebral cortex of *O. degus*. (*A* and *B*) Brain slices stained with Thioflavine S exhibited insoluble amyloid deposits (arrows) in the cerebral cortex (Cx) and in the hippocampus (Hip) of degus. Discrete numbers of plaques were observed in aged degus (72 mo-old; *B*, *B1*, and *B2*), but were almost absent in young animals (12 mo-old; *A*, *A1*, and *A2*). (*C* and *D*) Magnification of different morphological types of plaques found in the hippocampus showing diffuse (*C*) and dense (*D*) plaques in 60-mo-old and 72-mo-old degus, respectively. (*E*) Quantification of ThS burden (percentage of area occupied by Thioflavin S-positive plaques) for 6-mo-old (white; $n = 2$), 12-mo-old (gray; $n = 2$), 36-mo-old (blue; $n = 2$), 60-mo-old (red; $n = 2$), and 72-mo-old (black; $n = 2$) revealing a significant increase after 36 mo-old in cortex and after 60 mo-old in hippocampus. One-way ANOVA [$F_{(4,88)} = 48.64$, $^*P < 0.0001$ for ThS-Hip; $F_{(4,88)} = 63.44$, $^*P < 0.0001$ for ThS-Cx], followed by Tukey's post hoc test ($P < 0.05$) compared with 6 mo-old.

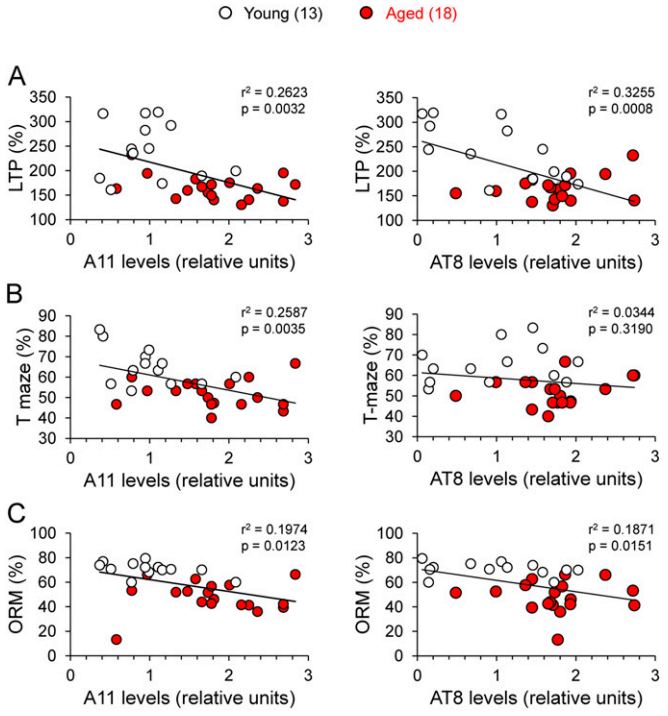

Fig. S4. Large soluble Aβ oligomers and tau phosphorylation are correlated with LTP and memory impairment in *O. degus*. Shown are relationships between LTP magnitude and A11 or AT8 tau phosphorylated epitope levels (*A*), between T-maze and A11 or AT8 tau phosphorylated epitope levels (*B*), and between ORM and A11 or AT8 tau phosphorylated epitope levels (*C*) for young and aged degus. The values in parentheses indicate the number of animals used.

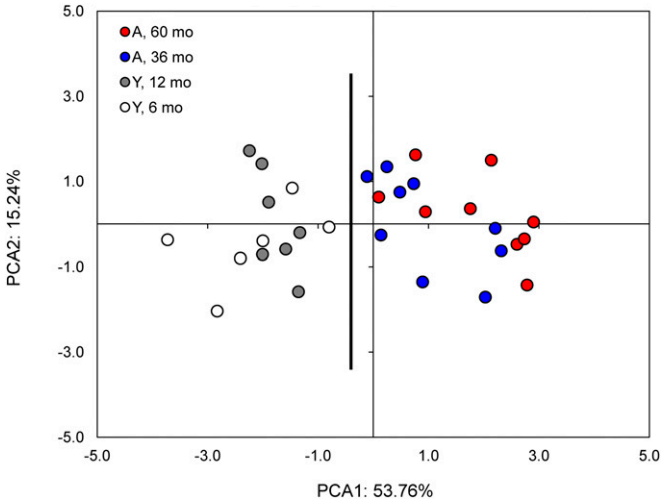

Fig. S5. Visualization and prediction with principal components analysis. The reduction of dimensionality can be applied down to dimension two, which is convenient for visualization of data with minimal loss of information (Tables S4 and S5). Subjects were segregated into two main classes (colored circles), which constitutes a reliable prediction concerning the range of age (young vs. old animals), here indicated by the solid line. Here 69% of the variance is explained by the first two principal components (Tables S4 and S5).

Table S1. Correlation matrix extract from the variables examined in this study

	Age	LTP	Tmaze	ORM	12 mer	9mer	6mer	4mer	3mer	A11	PHF-1	AT8	PSD-95	GluR2	NR2B	SYP
Age	1.00	−0.69	−0.60	−0.76	0.68	0.18	0.34	−0.14	0.19	0.63	0.61	0.45	−0.36	−0.55	−0.60	−0.08
LTP	−0.69	1.00	0.57	0.63	−0.56	−0.07	−0.38	0.21	−0.13	−0.51	−0.53	−0.57	0.20	0.33	0.37	−0.09
Tmaze	−0.60	0.57	1.00	0.73	−0.60	−0.16	−0.28	0.02	−0.14	−0.51	−0.44	−0.18	0.21	0.10	0.35	0.05
ORM	−0.76	0.63	0.73	1.00	−0.58	−0.15	−0.34	0.02	−0.08	−0.45	−0.61	−0.44	0.39	0.37	0.29	0.26
12mer	0.68	−0.56	−0.50	−0.58	1.00	0.40	0.61	0.14	0.41	0.52	0.77	0.42	−0.59	−0.22	−0.48	−0.24
9mer	0.18	−0.07	−0.16	−0.15	0.40	1.00	0.59	0.58	0.55	−0.03	0.42	−0.04	−0.58	0.09	−0.08	−0.44
6mer	0.34	−0.38	−0.28	−0.34	0.61	0.59	1.00	0.30	0.66	0.29	0.49	0.16	−0.61	−0.12	−0.30	−0.50
4mer	−0.14	0.21	0.02	0.02	0.14	0.58	0.30	1.00	0.12	−0.17	0.05	−0.10	−0.27	0.29	0.21	−0.33
3mer	0.19	−0.13	−0.14	−0.08	0.41	0.55	0.66	0.12	1.00	0.09	0.30	0.11	−0.53	−0.10	−0.32	−0.19
A11	0.63	−0.51	−0.50	−0.45	0.52	−0.03	0.29	−0.17	0.09	1.00	0.45	0.27	−0.19	−0.38	−0.37	−0.28
PHF-1	0.61	−0.53	−0.44	−0.61	0.77	0.42	0.49	0.05	0.30	0.45	1.00	0.62	−0.52	−0.27	−0.23	−0.26
AT8	0.45	−0.57	−0.18	−0.44	0.42	−0.04	0.16	−0.10	0.11	0.27	0.62	1.00	−0.24	−0.45	−0.08	0.12
PSD-95	−0.36	0.20	0.21	0.39	−0.59	−0.58	−0.61	−0.27	−0.53	−0.19	−0.52	−0.24	1.00	0.29	0.21	0.69
GluR2	−0.55	0.33	0.10	0.37	−0.22	0.09	−0.12	0.29	−0.10	−0.38	−0.27	−0.45	0.29	1.00	0.42	0.06
NR2b	−0.60	0.37	0.35	0.29	−0.48	−0.08	−0.30	0.21	−0.32	−0.37	−0.23	−0.08	0.21	0.42	1.00	−0.09
SYP	−0.08	−0.09	0.05	0.26	−0.24	−0.44	−0.50	−0.33	−0.19	−0.28	−0.26	0.12	0.69	0.06	−0.09	1.00

See *Principal Components Analysis* for further explanation.

Table S2. T-maze and ORM behavioral test results

Test	Young	Aged
ORM	(n = 13)	(n = 18)
Total no. of visits	17.8 ± 1.2	11.5 ± 0.7*
Latency to the first visit, s	10.1 ± 2.3	25.6 ± 3.2*
New object inspection time, s	31.1 ± 3.1	12.5 ± 1.2*
Familiar object inspection time, s	12.8 ± 1.9	10.7 ± 1.2
Total inspection time, familiarization, s	47.9 ± 5.7	20.2 ± 2.2*
T-maze	(n = 13)	(n = 18)
Latency to the first choice, s	12.7 ± 5.3	11.1 ± 4.7
No. of correct choices	6.6 ± 0.2	5.5 ± 0.1

Data are mean ± SEM.
*Statistical significance determined by ANOVA ($P < 0.0001$) compared with young group.

Table S3. Average data ± SD used for correlations and principal components analysis

Age, mo	LTP	Tmaze	ORM	12 mer	9mer	6mer	4mer	3mer	A11	PHF-1	AT8	PSD-95	GluR2	NR2B	SYP
60	153.4 ± 17.7	51.9 ± 7.6	44.2 ± 15.6	2.3 ± 0.3	1.6 ± 1.0	1.8 ± 0.5	1.3 ± 0.4	1.5 ± 0.8	3,632 ± 124	1.9 ± 0.7	1.2 ± 0.4	1.6 ± 1.8	0.6 ± 0.2	0.7 ± 0.2	5.4 ± 3.0
36	176.4 ± 27.6	51.9 ± 6.3	51.8 ± 7.9	2.1 ± 0.6	1.9 ± 0.9	1.7 ± 0.9	1.7 ± 0.7	1.4 ± 0.9	2,942 ± 1,041	1.7 ± 0.7	1.3 ± 0.4	2.2 ± 2.2	0.7 ± 0.2	0.8 ± 0.2	5.6 ± 3.1
12	241.1 ± 59.0	63.3 ± 7.2	68.6 ± 6.9	1.4 ± 0.3	0.9 ± 0.8	1.1 ± 0.5	1.2 ± 0.4	1.2 ± 0.9	2,280 ± 847	0.7 ± 0.4	0.8 ± 0.6	3.8 ± 2.6	0.9 ± 0.2	1.1 ± 0.3	7.2 ± 6.7
6	245.3 ± 62.5	67.8 ± 11.5	73.2 ± 2.6	1.6 ± 0.2	1.7 ± 1.0	1.3 ± 0.9	1.7 ± 1.0	1.0 ± 0.9	1,310 ± 644	0.9 ± 0.4	0.6 ± 0.3	3.1 ± 1.9	1.0 ± 0.2	1.2 ± 0.2	5.2 ± 4.4

Table S4. Principal components (PC1–PC7) for variables with correlation >0.5

	PC1	PC2	PC3	PC4	PC5	PC6	PC7
LTP	−0.41	0.04	0.11	−0.22	0.88	−0.01	0.03
Tmaze	−0.39	0.31	0.57	−0.11	0.28	0.50	−0.30
ORM	−0.44	0.16	0.11	−0.39	0.34	−0.63	0.33
Aβ*56	0.43	−0.10	0.31	−0.48	−0.03	0.33	0.61
PHF1	0.40	−0.21	0.60	−0.10	−0.11	−0.47	−0.45
GluR2	−0.24	−0.73	−0.24	−0.47	0.15	0.17	−0.29
NR2B	−0.30	−0.55	0.39	0.57	0.04	−0.01	0.37

Table S5. Variance explanation for the first four principal components

	% of total variance	Cumulative, %
PC1	53.8	53.8
PC2	15.2	69.0
PC3	10.3	79.3
PC4	9.9	89.2